Nonfouling Response of Hydrophilic Uncharged Polymers

*Ângela Serrano, Olof Sterner, Sophie Mieszkin, Stefan Zürcher, Samuele Tosatti, Maureen E. Callow, James A. Callow, and Nicholas D. Spencer**

Polymeric ultrathin films present a possible line of attack against marine biofouling for some applications. A protocol that provides a reliable comparison of the resistance of different polymers to biofouling is described. This is achieved through the use of a common, azide-terminated adhesion monolayer, to which different nonfouling polymers of various molecular weights, specifically poly(ethylene glycol) (PEG), poly(2-ethyl-2-oxazoline) (PEOXA), poly(vinyl pyrrolidone) (PVP), poly(vinyl alcohol) (PVA), and dextran are covalently bound. These functionalized surfaces are characterized by dynamic contact angle, ellipsometry, and X-ray photoelectron spectroscopy (XPS). To validate the developed protocol and evaluate performance against a selection of well-known, marine-fouling organisms, the nonfouling surfaces are subjected to a comparative biological study by exposure to a complex protein solution (with characterization via ellipsometry and quartz crystal microbalance with dissipation (QCM-D)), marine bacteria (*Cobetia marina* and *Marinobacter hydrocarbonoclasticus*), and zoospores of the green alga *Ulva linza*. The resulting data are used to draw conclusions on structure-property relationships. Chemical resistance towards marine fouling can be achieved using the described immobilization method, but is highly dependent on the species tested. Findings show that PVP (55 kDa)-coated surfaces display consistent resistance towards all tested solutions and organisms and, hence, this polymer could be considered as a potential material for marine-nonfouling applications.

1. Introduction

Fouling impairs the function of all structures immersed in seawater, including ship hulls, aquaculture nets, and static structures. Prevention of marine fouling represents an unsolved challenge with the potential for huge savings in terms of reduced energy consumption due to reduced frictional drag losses and weight, as well as increased life-time and maintenance intervals for exposed components.[1,2] The high level of complexity in the biointerfacial processes involved in biofouling, and the many different length and time scales[3] involved, characterize the difficulty in finding the most appropriate solution to the problem. Several strategies have been used in order to control fouling in the marine environment: besides a number of approaches to simplify the process of mechanical removal of the formed deposits, the use of antifouling paints incorporating biocides[4] is the most commonly employed approach. However, strategies that aim at the generation of passive, non-interacting, non-adhesive surface structures or coatings[5] are gaining more and more importance, and information gained from materials designed to combat fouling by proteins or biomedically important microorganisms are aiding the development of environmentally benign marine coatings.[6] The use of hydrophilic and uncharged polymers is often considered as a possible approach, and it has been shown that brush-forming polymers displaying hydration properties, that is, the capability to bind water around the polymer chain,[7,8] can be used to reduce the uptake of biological entities (e.g., macromolecules, cells, larvae) under various conditions. For example, the settlement (attachment) of zoospores of the marine alga *Ulva linza* and diatoms (unicellular slime-forming algae) and the adsorption of various proteins (fibrinogen, myoglobin, albumin, or full blood serum) have been shown to be significantly reduced on poly(ethylene glycol) (PEG)-coated surfaces,[6,9,10] as well as on polymeric coatings incorporating PEGylated moieties;[11–13] the polymer poly(2-ethyl-2-oxazoline) (PEOXA) has been studied as a liposomal surface modifier for drug-delivery vesicles with an efficiency similar to PEG,[14] but has also been shown to be resistant to bovine serum albumin (BSA) adsorption;[15] poly(vinyl pyrrolidone) (PVP) has been shown to decrease fouling by lysozyme, BSA and fibrinogen;[16–18] poly(vinyl alcohol) (PVA) was found to be effective in reducing the adhesion of the diatom *Amphora coffeaeformis* independently of the shear rate the surfaces were subjected to,[19] and as a gel has been shown to reduce barnacle attachment;[20,21] and dextran has shown the ability to reduce adsorption of human-serum proteins.[22,23]

Â. Serrano, O. Sterner, Dr. S. Zürcher, Dr. S. Tosatti, Prof. N. D. Spencer
Laboratory for Surface Science and Technology
Department of Materials
ETH Zurich, Wolfgang-Pauli Str. 10
CH-8093 Zurich, Switzerland
E-mail: nspencer@ethz.ch
Â. Serrano, Dr. S. Zürcher, Dr. S. Tosatti
SuSoS AG, Lagerstrasse 14, CH-8600 Dübendorf, Switzerland
Dr. S. Mieszkin, Dr. M. E. Callow, Prof. J. A. Callow
School of Biosciences
University of Birmingham, B15 2TT, UK

DOI: 10.1002/adfm.201203470

Besides the ability of a polymer to hydrate, the conformation of the polymer chain at the surface has also been found to correlate with the fouling resistance.[24] The so-called "brush regime" is known to result from high surface chain density of grafted polymers, when in the presence of a good solvent.[25] In order for a polymer to reach this conformation, the distance between anchoring sites has to be smaller than twice the radius of gyration of free polymer chains ($L < 2R_g$).[26] In general, two methods have been developed to fabricate polymer brushes on flat surfaces: the "grafting-to" and "grafting-from" techniques. In the former, end-functionalized polymer chains are end-tethered to a solid substrate via a chemical reaction. The formation of such coatings by adsorption is limited by the diffusion kinetics of free chains attempting to attach to an increasingly crowded surface. Thus, this approach normally results in a lower grafting density when compared to the "grafting-from" method, in which chains are grown from the substrate by surface-initiated polymerization techniques (e.g., atom-transfer radical polymerization (ATRP), nitroxide-mediated polymerization (NMP), reversible addition-fragmentation chain-transfer polymerization (RAFT)).[27,28] A higher grafting density is reached with grafting from, since the small monomer units more easily access the growing end of the chain. Challenges of the approach are to be found in potentially long reaction times, the complexity and control of the reaction due to oxygen sensitivity, and solution-versus-surface polymerization.

An alternative approach to achieving brush-like conformations on surfaces is the deposition and subsequent immobilization of a polymer chain onto a surface that has been functionalized with a primer layer containing reactive chemical entities, such as azides[29] or benzophenones.[30] Azides are known to possess the ability to decompose into nitrenes upon thermal or photo activation.[31,32] Nitrenes are highly reactive, short-lifetime chemical species that undergo various reactions such as cycloaddition, rearrangements or, most importantly for this work, insertion reactions.[33] Aryl azides have been widely used due to their high stability and, when halogenated, preferential formation of the required singlet nitrene intermediate that preferentially inserts, unspecifically, into C–H and N–H bonds,[34] rather than the alternative reactions of hydrogen abstraction or ring expansion taking place. The existence of this latter conformation would pose a problem, since it mainly reacts with nucleophiles such as amines, substantially decreasing the yield of products resulting from C–H insertion.[35] Examples of applications of this approach are: crosslinking,[36] photolabeling,[37] photolithography,[32] and surface modification.[38] In this work, the azide layer is used to generate multi-tethered polymer brushes that are monomolecular in thickness.

The aim of this work was to attach the above-mentioned hydrophilic, uncharged polymers (i.e., PEG, PVA, PEOXA, PVP) and dextran (**Figure 1**), onto a surface using the same modification procedure, and to study the existence of parameters that determine the overall capacity to resist marine fouling on different length and time scales. This developed system allows a reliable comparison between the efficiency of different nonfouling polymers. The approach was realized by means of a monolayer that possesses a cationic polymeric backbone and pendant azide groups (**Figure 2**). The backbone allows an electrostatic interaction to be formed with a negatively charged

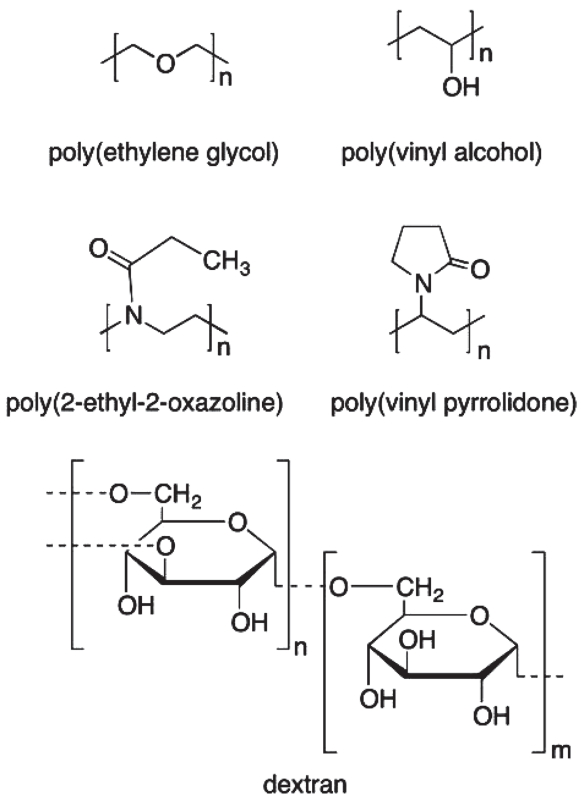

Figure 1. Chemical structures of the hydrophilic uncharged polymers used.

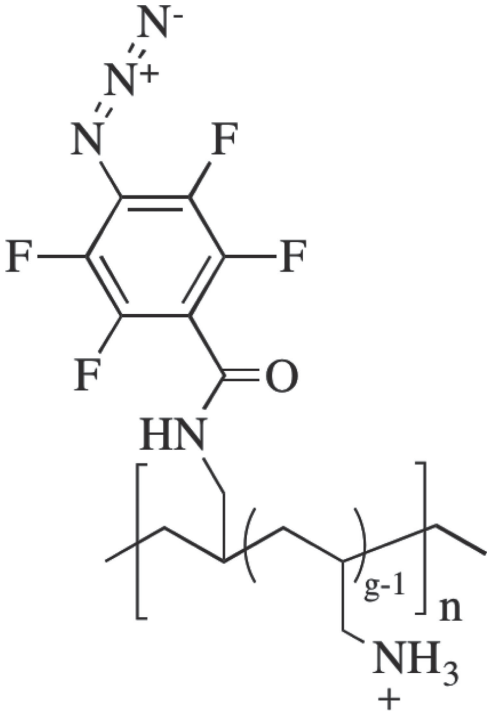

Figure 2. Chemical structure of poly(allylamine)-grafted-perfluorophenylazide (PAAm-g-PFPA).

substrate. Nitrenes formed from the azides following thermal or photo activation readily form covalent bonds with any organic matter in their close proximity.

The modified surfaces were then characterized by means of variable-angle spectroscopic ellipsometry (VASE), X-ray photoelectron spectroscopy (XPS), dynamic water contact angle (dCA) and quartz-crystal microbalance with dissipation (QCM-D). Further comparative biological studies were performed by exposure of the coated samples to a complex protein solution (full human serum), so that nonspecific protein adsorption could be evaluated, two marine bacteria (*Cobetia marina* and *Marinobacter hydrocarbonoclasticus*) and zoospores of the marine alga *Ulva linza*. Spores of *U. linza* are motile pyriform cells, 7–8 μm length, which must locate and settle (permanently adhere) on a surface, in order to complete their life cycle.[39] Spores respond to a variety of surface-associated cues and have been extensively used in comparative assays of the antifouling performance of experimental coatings.[3] The approach adopted in the research reported here allowed the newly developed surface-functionalization protocol to be validated and performance evaluated against a selection of well-known fouling organisms.

2. Results

2.1. Surface Characterization

The adlayer thickness, the contact angle and the chemical composition of the different coatings, and of the freshly cleaned substrate and a UV-activated adhesion promoter (PAAm-g-PFPA) film, were measured by VASE, dCA, and XPS, respectively. For XPS, detail spectra for Si 2p, C 1s, O 1s, N 1s, and F 1s were measured, to determine the apparent atomic composition of the deposited films. Peak modeling allowed the contributions from the silicon oxide and the elemental silicon to be discerned, and the oxygen contribution from the SiO_2 substrate to be calculated. Subtraction of this value allowed the atomic composition of the polymeric films to be calculated and compared with the theoretical composition of the pure polymer (see results in **Table 1** and experimental parameters in **Table 2**). Peak modeling also enabled the C 1s signal to be deconvoluted into its various contributions. Their relative peak areas were compared to the theoretical carbon compositions of the analyzed films (see **Table 3**).

2.1.1. Si-Wafer and Adhesion Promoter

The freshly cleaned substrate was characterized by a high surface energy (low contact angle) and the presence of elemental silicon, oxidized silicon as interfacial SiO and SiO_2, oxygen, and a small amount of adventitious carbon contamination. No other elements, specifically nitrogen or fluorine, were detected.

The successful deposition of the adhesion promoter (Figure 2) onto Si-wafers could be confirmed by an increase in carbon, the presence of nitrogen and fluorine, and the subsequent decrease of silicon and oxygen as a consequence of a 1.8 ± 0.1 nm thick adlayer. Due to the presence of the PFPA groups, an increase in advancing contact angle value of 43° with respect to bare silicon was also observed (Table 1).

Upon subtraction of the silicon and silicon oxide contributions, the film composition of the adhesion promoter differs from the theoretically calculated stoichiometry. From the F/N ratio, an effective grafting ratio of 9.0 for PAAm-g-PFPA can be calculated, where grafting ratio is defined as the number of allylamine monomer units divided by the number of PFPA units. The main deviation is an increased oxygen content (real composition of 20 ± 2 at.% and a theoretical composition of 2.0 at.%), which can be attributed to deprotonated surface hydroxyl anions. These must be present for charge neutralization of the positively charged ammonium groups of the adhesion promoter.

2.1.2. Nonfouling Polymeric Adlayers

The deposition of nonfouling polymers was also confirmed by the same three techniques. Overall, an increase in film thickness and decrease in dCA (Table 1) was measured when compared to the adhesion-promoter layer. Dynamic water contact angles ranged from 19° to 46° (advancing) and <10° to 23° (receding). The decrease in advancing contact angle of the new layer, when compared to the adhesion promoter, is due to the hydrophilicity of the newly bound polymers. Also, the relatively small hysteresis (between 14° and 24°) indicates a smoother and more homogeneous layer than for the adhesion promoter alone.

These changes in hydrophilicity throughout the various functionalization steps were accompanied by a sequential increase in dry thickness. PEOXA, PVA, and PVP 55 are among the thinnest layers with values of 0.6 ± 0.3 nm, 0.9 ± 0.3 nm, and 1.9 ± 0.3 nm, respectively, while dextran and PVP 1300 have layers of 7.1 ± 0.7 nm and 11.6 ± 0.9 nm, which is consistent with the trend in the molecular weight of the polymers.

Regarding chemical composition (Table 1), the deposited PVA can be clearly detected by an increase in the **C**–O component in the C 1s detail spectrum when compared to the adhesion promoter (**Figure 3**). Due to this thin deposited layer, nitrogen and fluorine are still detected, explaining the deviations from the calculated PVA stoichiometry. This fact is also verified in Table 3 where an approximate contribution of 5% of all carbon content was due to the presence of groups such as **C**=O or **C**–F.

The thicker (3.9 ± 0.6 nm) PEG coating behaved similarly to PVA, showing an overall increase of carbon, oxygen, and a marked augmentation of the **C**–O peak due to the ether bond (Figure 3). The existence of other types of carbon (Table 3), as well as an overestimation of the film's stoichiometry (Table 1), is an indication that the adhesion-promoter layer is again contributing to the measured film composition.

In the case of dextran, the substrate signal is mostly masked by the 7.1 ± 0.7 nm layer consisting of carbon and oxygen, which matches well the theoretical composition. The bond between the polymer and the adhesion promoter is confirmed by data obtained from the C 1s peak deconvolution (see Table 3), where there is an increase in concentration of **C**–OH and O–**C**–O/**C**=O, confirming the successful attachment of this polysaccharide. The relatively high content of the latter peak, as observed in all chemistries described so far, can be attributed to the presence of the adhesion promoter.

Table 1. Surface characterization of the substrate (silicon with naturally grown SiO_2 layer), the adhesion promoter layer after activation, and the six investigated polymer films. The samples were characterized by dynamic water contact angle (dCA), the film thicknesses were determined by VASE and the apparent normalized atomic concentrations were measured by XPS. In the case of the polymer films, the compositions were determined by subtraction of the silicon and silicon oxide contributions. Calculated polymer compositions are given in brackets for comparison. For the adhesion promoter, a grafting ratio of g = 9 was used, as calculated from the F/N ratio. Changes in film thickness after immersion in artificial seawater (ASW) for 1 h at room temperature were measured by VASE as an indication of the coating stability under these conditions. Errors correspond to standard deviation (±SD) of at least three independent measurements, on different samples.

Chemistry	Surface characterization									Stabilization in ASW
	dCA	VASE		XPS						VASE
	Adv [°]	Rec [°]	Thickness [nm]		Si 2p	C 1s	O 1s	N 1s	F 1s	Thickness change after 1h immersion in ASW [nm]
SiO_2	27 ± 2	12 ± 1	-	At.%	34.8 ± 0.1	4.3 ± 0.3	60.9 ± 0.3	0.0 ± 0.0	0.0 ± 0.0	-
PAAm-g-PFPA (activated, and with a grafting ratio of 9)	70 ± 1	19 ± 1	1.8 ± 0.1	At.%	25.3 ± 0.2	24.5 ± 0.6	43.4 ± 0.7	4.9 ± 0.3	1.9 ± 0.1	Δ = 0.2 ± 0.2
				Normalized at.% (overlayer)		63 ± 1 (69.4)	20 ± 2 (2.0)	12.5 ± 0.6 (20.4)	5.0 ± 0.2 (8.2)	
PVA 27 kDa	41 ± 1	17 ± 1	0.9 ± 0.3	At.%	17.0 ± 0.7	42.1 ± 0.7	37.4 ± 0.2	2.4 ± 0.3	1.1 ± 0.0	Δ = –0.4 ± 0.3
				Normalized at.% (overlayer)		67.8 ± 0.8 (66.7)	26.5 ± 1.0 (33.3)	3.9 ± 0.5 (0.0)	1.8 ± 0.0 (0.0)	
PEG 20 kDa	29 ± 2	15 ± 1	3.9 ± 0.6	At.%	8.6 ± 0.1	56.7 ± 0.3	32.6 ± 0.1	1.5 ± 0.2	0.7 ± 0.1	Δ = –2.2 ± 0.4
				Normalized at.% (overlayer)		70.6 ± 0.4 (66.7)	26.7 ± 0.2 (33.3)	1.8 ± 0.2 (0.0)	0.8 ± 0.2 (0.0)	
Dextran 2000 kDa	19 ± 2	<10	7.1 ± 0.7	At.%	2.6 ± 0.2	55.8 ± 0.3	41.6 ± 0.2	0.0 ± 0.0	0.0 ± 0.0	Δ = –0.4 ± 0.2
				Normalized at.% (overlayer)		58.0 ± 0.2 (54.5)	42.0 ± 0.2 (45.5)	0.0 ± 0.0 (0.0)	0.0 ± 0.0 (0.0)	
PEOXA 50 kDa	46 ± 1	23 ± 1	0.6 ± 0.3	At.%	18.3 ± 0.6	42.2 ± 0.6	29.9 ± 0.3	8.4 ± 0.3	1.1 ± 0.1	Δ = –0.1 ± 0.2
				Normalized at.% (overlayer)		72.0 ± 0.7 (71.4)	11.8 ± 0.2 (14.3)	14.4 ± 0.4 (14.3)	1.9 ± 0.2 (0.0)	
PVP 55 kDa	35 ± 2	14 ± 1	1.9 ± 0.3	At.%	8.5 ± 0.6	63 ± 1	17.9 ± 0.7	9.9 ± 0.1	0.6 ± 0.2	Δ = –0.2 ± 0.2
				Normalized at.% (overlayer)		78.5 ± 0.4 (75.0)	8.5 ± 0.3 (12.5)	12.3 ± 0.0 (12.5)	0.7 ± 0.2 (0.0)	
PVP 1300 kDa	35 ± 1	12 ± 3	11.6 ± 0.9	At.%	0.8 ± 0.1	76.6 ± 0.3	10.7 ± 0.2	11.9 ± 0.3	0.0 ± 0.0	Δ = –0.2 ± 0.2
				Normalized at.% (overlayer)		77.9 ± 0.4 (75.0)	9.9 ± 0.2 (12.5)	12.1 ± 0.2 (12.5)	0.0 ± 0.0 (0.0)	

In the case of PEOXA, when comparing the chemical composition with the adhesion promoter, one can observe a decrease of fluorine given by the presence of an overlayer and an increase of both nitrogen and **C**–N contributions in the carbon region, as expected from the chemical structure of this polymer. Attachment of both PVPs translated also into an increase in the nitrogen atomic percentage along with carbon. The normalized values are very close to the expected stoichiometry, where a fourth carbon peak attributed to the alpha carbon was found to be necessary to create a reasonable fit.

2.2. Short-Term Stability of Coatings

Table 1 gives the change in resulting adlayer thickness after short-term exposure (1 h) to artificial seawater (ASW). The data show how the exposure to ASW, a high-ionic-strength medium, caused an overall reduction of the thickness of the coatings. The less-affected chemistries with a decrease below 11.1% were the adhesion promoter, both PVPs and dextran. PVA and PEOXA suffered a reduction of thickness of the order of 44.4% and 16.7%, respectively, while PEG decreased in thickness by 56.4%. One possible reason for the reduction of PEG thickness is the formation of a hydrolytically unstable bond upon nitrene insertion into C–H bonds of the PEG. However, with the exception of this last chemistry, all thickness variations are comparable to the standard deviation so that, with exception of PEG, no statistical relevance between fresh and exposed films could be determined. This suggests that the coatings are stable in the short term (1 h) and that fouling events can be correlated to an interaction between species and coating material, rather than to an exposure of adhesive bare substrate due to coating loss. A control substrate (bare SiO_2) was simultaneously tested but, as expected, no changes in thickness were observed.

2.3. Biofouling Assessment

The results for protein resistance, attachment of marine bacteria, *C. marina* and *M. hydrocarbonoclasticus*, and settlement

Table 2. XPS Binding energies and peak-deconvolution parameters. Data shown are average ± standard deviation.

Element	Assignment	BE	FWHM	Constraints	Line Shape	RSF
C 1s	C–C, C–H	285.0 ± 0.0	1.4 ± 0.2	none	GL(30)	1
	C–C = O	285.5 ± 0.1	1.3 ± 0.1	FWHM C1s aliphatic 1*area (C–F, C = O);	GL(30)	1
	C–N, C–O	286.4 ± 0.4	1.4 ± 0.2	FWHM C1s aliphatic	GL(30)	1
	C–F, C = O	287.9 ± 0.2	1.4 ± 0.1	FWHM C1s aliphatic	GL(30)	1
O 1s	(N)C = O	531.3 ± 0.5	1.5 ± 0.3	none	GL(50)	2.642
	SiO_2, C–OH, C–O–C	532.8 ± 0.3	1.5 ± 0.1	none	GL(50)	2.642
N 1s	N–H	399.7 ± 0.2	1.6 ± 0.2	none	GL(30)	1.721
	(O = C)–N	401.7 ± 0.2	1.6 ± 0.2	FWHM (N–H)	GL(30)	1.721
F 1s	C–F	688.0 ± 0.1	1.8 ± 0.2	none	GL(30)	3.672
Si 2p	Si $2p_{3/2}$	98.4 ± 0.3	0.8 ± 0.1	none	GL(30)	0.872
	Si $2p_{1/2}$	99.1 ± 0.3	0.8 ± 0.1	FWHM (Si $2p_{3/2}$); 0.5*area (Si $2p_{3/2}$); BE = BE(Si $2p_{3/2}$)+0.7	GL(30)	0.436
	SiO $2p_{3/2}$	100.3 ± 0.3	1.4 ± 0.2	none	GL(30)	0.872
	SiO $2p_{1/2}$	101.0 ± 0.3	1.4 ± 0.2	FWHM (SiO $2p_{3/2}$); 0.5*area (SiO $2p_{3/2}$); BE = BE(SiO $2p_{3/2}$)+0.7	GL(30)	0.436
	SiO_2 $2p_{3/2}$	102.7 ± 0.3	1.4 ± 0.1	none	GL(30)	0.872
	SiO_2 $2p_{1/2}$	103.4 ± 0.3	1.4 ± 0.1	FWHM (SiO_2 $2p_{3/2}$); 0.5*area (SiO_2 $2p_{3/2}$); BE = BE(SiO_2 $2p_{3/2}$)+0.7	GL(30)	0.436

BE: Binding energy; FWHM: Full width at half maximum; RSF: Relative sensitivity factor.

(attachment) of spores of *U. linza* are all presented in **Table 4**. In order to allow a direct comparison between all values, these have been normalized with respect to the positive control SiO_2 (100%) and are displayed in **Figure 4**.

2.3.1. Human Serum

To evaluate protein resistance of the developed surfaces, a solution of human serum was used. While human serum may seem to be a surprising choice for testing surfaces for marine biofouling applications, it has the advantage of being well characterized, containing a wide range of proteins, and being readily available. Protein uptake, both on bare and functionalized surfaces, was studied using two different techniques: ex situ ellipsometry and QCM-D. The first technique gives information regarding the dry thickness, or dry mass, and measurements were performed before and after protein exposure. It is characterized with a thickness resolution of 0.1–0.2 nm. The latter method, QCM-D, can provide information regarding polymer conformation, via associated water content and film thicknesses.[40–44] It is highly sensitive to the absorbed mass, and allows in situ real-time monitoring. It has a mass sensitivity of about 5 ng cm^{-2} and measures both changes in frequency and dissipation of the oscillating system. Through the Sauerbrey Equation, the frequency shift (Δf) can be related to the adsorbed mass per unit area (Δm):

$$\Delta m = -C \times \frac{\Delta f}{n} \quad (1)$$

C is the sensitivity constant of the quartz crystal with a value of 17.7 ng cm^{-2} Hz^{-1} and n is the overtone number. This calculated acoustic mass comprises the mass associated with the adsorbed protein together with the water bound to those proteins (hydration via molecule entrapment and/or hydrodynamic coupling).

Ellipsometry results show that the protein uptake was maximal for the bare SiO_2 substrates, showing an increase in thickness of 3.7 nm, corresponding to a dry mass of 546.9 ng cm^{-2}, while with QCM-D it was measured as a hydrated uptake of 850 ng cm^{-2}. All other chemistries, including the more hydrophobic adhesion promoter, revealed a substantial decrease in the uptake, confirming the nonfouling nature of the studied polymers. The values for ex situ analysis show that the best

Table 3. Normalized C 1s content. The theoretical carbon compositions of the polymer films are given in parentheses, for comparison. Data shown are average ± standard deviation.

Chemistry	Relative peak area (%)			
	C–C, C–H	C–C=O	C–O, C–N	O–C–O, C=O, C–F
SiO_2	74 ± 5	-	26 ± 5	-
PAAm-g-PFPA	61 ± 3 (52.9)	-	23 ± 3 (32.4)	16.7 ± 0.8 (26.3)
PVA 27 kDa	49.9 ± 0.5 (50)	-	45.2 ± 0.9 (50)	4.8 ± 0.4 (0.0)
PEG 20 kDa	7 ± 1 (0.0)	-	86 ± 3 (100)	7 ± 2 (0.0)
Dextran 2000 kDa	5.0 ± 0.3 (0.0)	-	71 ± 2 (83.3)	24 ± 2 (16.7)
PEOXA 50 kDa	37 ± 1 (40)	-	43.0 ± 0.9 (40)	19.8 ± 0.5 (20)
PVP 55 kDa	34 ± 3 (33.3)	16.8 ± 0.6 (16.7)	32 ± 2 (33.3)	16.8 ± 0.6 (16.7)
PVP 1300 kDa	31 ± 3 (33.3)	16.6 ± 0.2 (16.7)	36 ± 3 (33.3)	16.6 ± 0.2 (16.7)

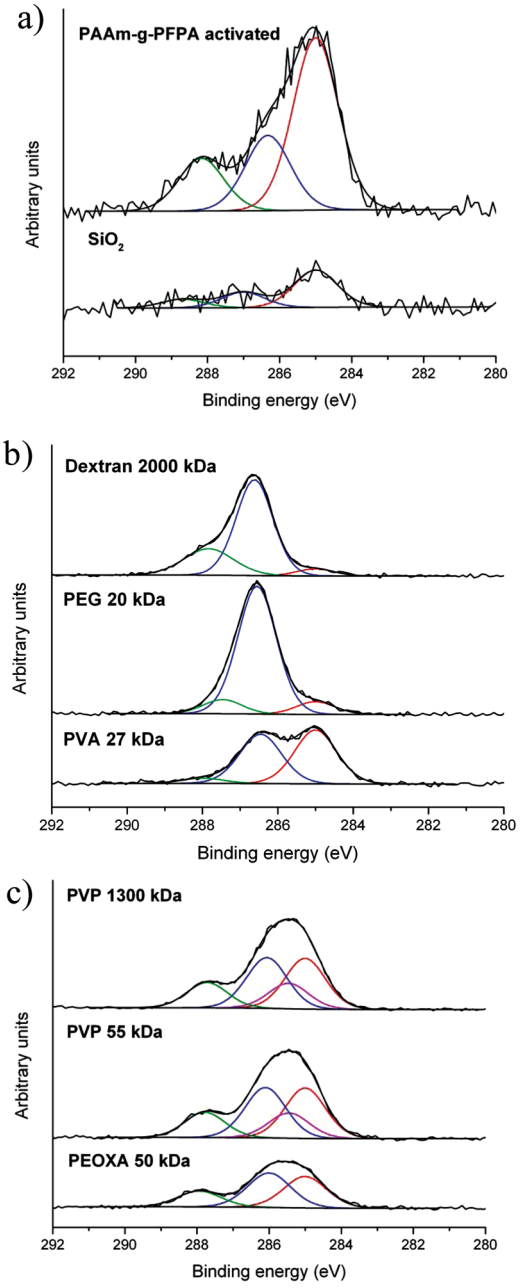

Figure 3. Detailed XPS spectra of the C 1s region on the bare SiO_2 and various functionalized surfaces. Curve-fitted carbon component C–C, C–H in red; C–C=O in pink; C–N, C–O in blue and C–F, C=O in green (details in Table 3).

results were obtained for PEG, PVA, and dextran, although there was no statistical difference from all the other nonfouling surfaces with the exception of PVP 55 kDa. The statistical similarity for PEG, PVA, and dextran is not observed in the QCM studies, but PEG and the hydroxylated PVA and dextran still show extremely low uptake in in situ measurements, validating the trend observed with ellipsometry. It also suggests that high-molecular-weight PVP has an increased protein resistance in situ when compared to the values given by the former technique. But in the case of the already quite thick PVP film, the difference measured by ellipsometry of 0.5 ± 0.2 nm is not relevant, since the dry film thickness before exposure to protein varies by ±0.9 nm. These variations are not taken into account in the in situ QCM-D measurement and, therefore, we also consider the high-molecular-weight PVP as being fully protein resistant.

2.3.2. Marine Bacteria

Two strains of bacteria were used, since they have been reported to present different surface energies: *Cobetia marina* has been considered hydrophilic, while *Marinobacter hydrocarbonoclasticus* is a hydrophobic species.[45]

Results show that some differences in attachment do exist between the two species (Table 4 and Figure 4). Exposure to *C. marina* leads to a significantly higher number of attached bacteria on the adhesion promoter (11 086 ± 102 bacteria per mm^{-2}) than on the bare SiO_2 control (7606 ± 85 bacteria per mm^{-2}). The remaining functionalized surfaces showed a considerable decrease in cell attachment whereas PVA, PEG, and dextran-containing chemistries showed the lowest number of bacteria per unit area with over 90% decrease in attachment and there was no statistical difference between them. Regarding *M. hydrocarbonoclasticus,* the data show equally high attachment on the adhesion-promoter-coated surface (12 000 ± 29 bacteria per mm^2), with a significant decrease in attachment on almost all other surfaces, including bare SiO_2. The unexpected result here is the surface modified with dextran, on which a high attachment of *M. hydrocarbonoclasticus* was obtained (9034 ± 28 bacteria per mm^2). One common result between both strains is the surface leading to minimum settlement: PEG was characterized by 90 ± 6 and 182 ± 4 bacteria per mm^2 for *C. marina* and *M. hydrocarbonoclasticus*, respectively. However, these values were not significantly different (one-way ANOVA, $p < 0.05$) from the next best performing surfaces for either species, (hydroxylated PVA and Dextran in the case of *C. marina*, PEOXA and PVP 55kDa in the case of *M. hydrocarbonoclasticus*).

2.3.3. Zoospores of U. Linza

By comparing settlement of zoospores between surfaces, it can be observed that a significant decrease was achieved on the substrates functionalized with hydrophilic polymers, compared with the bare SiO_2 surface (Table 4 and Figure 4). The same did not occur on the slightly more hydrophobic adhesion-promoter layer where 689 ± 60 spores per mm^2 were attached versus the 595 ± 93 spores per mm^2 that characterized the bare SiO_2. The PEG-functionalized surface showed a significantly higher settlement of zoospores than expected, with 365 ± 99 zoospores per mm^2. This can be a consequence of stability issues associated with this polymer, namely its thermal/oxidative degradation,[46] which were already observed in the study performed in Section 3.2. The hydroxylated chemistries of PVA and dextran appeared to be extremely resistant to the settlement of spores, with a settlement density of 24 ± 10 and 2 ± 1 spore per mm^2, respectively. Nevertheless, according to Tukey test, they were not statistically different from the nitrogen-containing chemistries of PEOXA and both PVPs.

Table 4. Results of all bioassays performed on test surfaces are shown (±95% confidence interval, one-way ANOVA).

Chemistries	Human serum uptake[1,2]		Marine bacteria[1,3]		Spores of U. linza[1,4]
	VASE	QCM-D	Cobetia marina	Marinobacter hydrocarbonoclasticus	Number of settled spores per mm^2
	Thickness [nm]	Δm [ng cm^{-2}]	Attached bacteria per mm^2	Attached bacteria per mm^2	
SiO_2	3.7 ± 0.1[a)]	850 ± 63[a)]	7606 ± 809[a)]	5320 ± 442[a)]	595 ± 96[a)]
PAAm-g-PFPA	1.9 ± 0.1[b)]	381 ± 70[b)]	11 086 ± 966[b)]	12 000 ± 279[b)]	689 ± 62[a)]
PVA 27 kDa	0.2 ± 0.2[c)]	80 ± 8[c,e)]	465 ± 123[c,e)]	3167 ± 550[c)]	24 ± 11[b)]
PEG 20 kDa	0.1 ± 0.3[c)]	–45 ± 26[d)]	90 ± 57[e)]	182 ± 38[e)]	365 ± 102[c)]
Dextran 2000 kDa	0.2 ± 0.1[c)]	65 ± 12[c,d,e)]	215 ± 53[e)]	9034 ± 270[f)]	2 ± 1[b)]
PEOXA 50 kDa	0.3 ± 0.1[c)]	333 ± 53[b)]	1708 ± 249[c,d)]	448 ± 55[e)]	42 ± 10[b)]
PVP 55 kDa	0.8 ± 0.1[d)]	177 ± 86[e)]	1601 ± 364[c,d)]	340 ± 57[e)]	82 ± 10[b)]
PVP 1300 kDa	0.5 ± 0.2[c,d)]	–12 ± 10[c,d)]	2736 ± 889[d)]	3131 ± 302[c)]	39 ± 5[b)]

[1)]The letters in brackets indicate significant differences ($p < 0.05$) using one-way ANOVA and a pairwise Tukey comparison test. Values with the same letter are not significantly different; [2)]At least four samples for each test surface were used to calculate the means and errors; [3)]Means obtained are based on 90 counts; 30 from each of three replicates per test surface; [4)]Means obtained are based on 90 counts; 30 from each of three replicates per test surface. A second set of test surfaces was used to validate these results by obtaining the same trend in resistance (data not shown).

3. Discussion

We have developed both a highly versatile surface-functionalization method and a comparative protocol for investigating the influence of different surface chemistries on different fouling stages, from proteins to cells, over different length scales (nm to μm for protein and bacteria/spores, respectively). Different coatings provided different relative responses, depending on the fouling species. In order to determine if those differences are material (chemistry) or architecture (conformation) dependent, we first need to build a conceptual model for our coatings.

3.1. Study of Novel Multiply Tethered Polymer Coatings

The conformation of the organic layer that is created via azide chemistry and described in this work is primarily determined by two factors. The first one is related to the polymeric backbone, PAAm-g-PFPA, which spontaneously adsorbs onto the SiO_2 surface due to an electrostatic interaction between the positively charged amine groups of the polymer and negatively charged deprotonated silanol groups of the silicon oxide substrate. The use of polyelectrolytes adsorbed on oppositely charged substrates is a well-known strategy that has found applications in such diverse areas as lubrication,[47] colloidal stabilization,[48] wetting,[49] or resistance to protein adsorption.[50] In order to better control the adsorption stability of polyelectrolytes, factors such as pH and ionic strength were optimized. To guarantee full coverage, physiological pH (7.4) was used, since this value lies between the isoelectric point of the substrate (1.7–3.5) and the pK_a of polyallylamine (9.5), providing a negatively charged substrate and a positively charged polymer backbone. The role that ionic strength plays is related to the conformation adopted by the polymer when adsorption occurs. At lower ionic strength, polyelectrolytes tend to adopt an extended conformation due to the high repulsion between the charged groups. By slightly increasing ionic strength, the polymer adopts a coiled configuration, due to reduced repulsion between charges, allowing more macromolecules to be adsorbed. By further increasing ionic strength, electrostatic screening between charges on the polymer and on the surface increases, and consequently adsorption is reduced. In the reported case, a low-ionic-strength medium (HEPES I–10 mM) is used for adsorption, which results in a planar conformation of our adsorbed polymeric backbone,[51] as confirmed by the measured thickness.

The second conformational condition is schematically represented in **Scheme 1**. Upon activation, the azide groups of the backbone will covalently bind to random segments of the polymer adlayer via insertion reactions. Three different situations for the bound polymer chain can be postulated: loops, trains, and/or tails. The first consists of unbound segments that are further away from the surface but are constrained by neighboring bonded segments; the second consists of successive bonds to the polymeric backbone; the third is when a sequence of bonded polymer (either in the configuration of a train or a loop) has one or both free chain ends stretched away from the surface.[52] This resembles the frequently used loop-train-tail model for adsorbed polymers.[53]

Literature on architectural studies of polymer brushes is fully based on end-grafted entities. A few theoretical studies have been performed on double-tethered brushes[54,55] but, due to its complexity, no work has been done so far on multi-tethered ones. The aim of this paper is not to provide a fundamental study on the behavior and limitations of this new class of brushes, as both the random nature of the nitrene insertion and the difficulty to experimentally distinguish between loops, trains, or tails does not allow a reliable quantitative study. Nevertheless, by using a simplified model in which only loops are considered, structure–property relationships can be compared with those of end-tethered polymer brushes and possible advantages and/or disadvantages can be extrapolated. To this end, and based on the proposed model, the equations

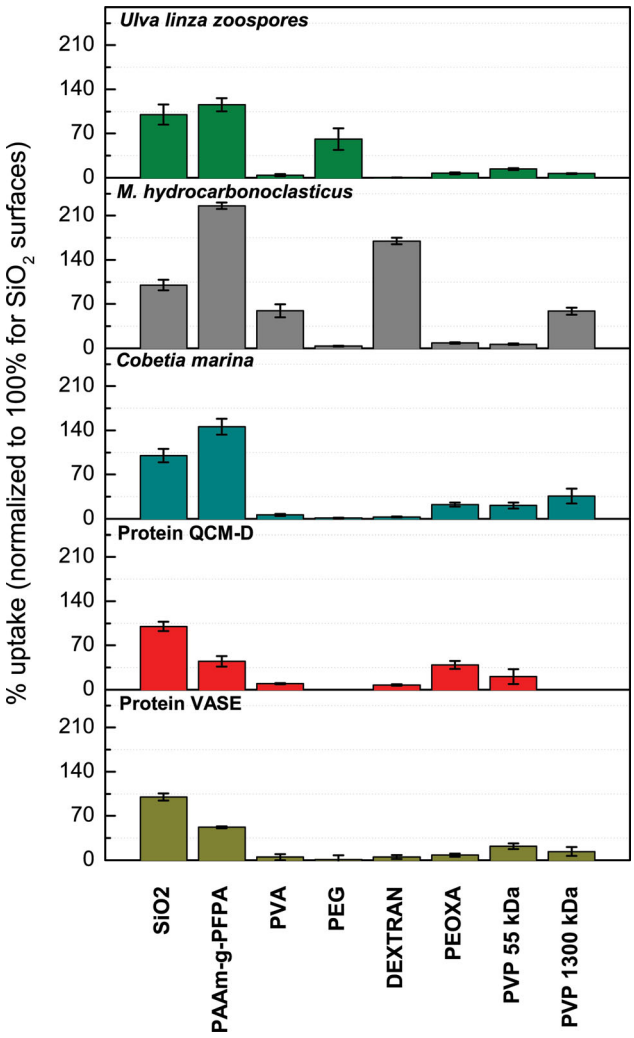

Figure 4. Normalized uptake results for tested nonfouling polymers regarding protein adsorption (provided by both VASE and QCM-D), bacteria (both *C. marina* and *M. hydrocarbonoclasticus*) and settlement of zoospores of *U. linza*. All data have been normalized against the results obtained from the bare SiO_2 (set to 100%).

for the physicochemical properties presented in **Table 5** have been deduced and calculated (more detail is provided in the Supporting Information) in order to obtain the final parameter $L_{id}/2R_c$, which correlates average distance between attachment points (L_{id}) and coiled radius of a collapsed loop (R_c).

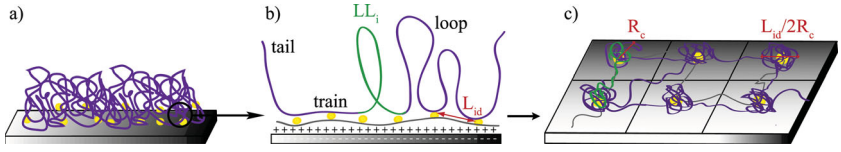

Scheme 1. a) Expected polymer architecture, b) simplified model, and c) the multi-tethered system described in this work, in which loops, trains and/or tails can be formed. For each surface attachment point, an average loop length LL_i can be calculated, from which the radius for a collapsed sphere R_c and the overlap of these polymer spheres on the surface, described by the parameter $L_{id}/2R_c$, can be determined, where L_{id} corresponds to the average distance between attachment points.

When correlating R_c with the distance between chains of grafted polymer (L_{id}), the regimes in which these loops are found can be directly compared to those that an end-tethered polymer brush can adopt. This is because, in a similar way, if one increases the surface density of loops, these will tend to stretch away from the surface in good solvent once the compensation between osmotic (excluded-volume effect) and elastic (stretching entropy) pressure is reached. Since $L_{id}/2R_g$ (where R_g is the radius of gyration of the polymer chains in good solvent) is an indicator of the potential for forming brushes on the surface, $L_{id}/2R_c$ can be used as an upper limit of this quantity, since the polymer will swell upon exposure to solvent, that is, $R_g > R_c$. Therefore, mirroring the generally accepted guidelines for $L_{id}/2R_g$, a conservative condition for brush formation is $L_{id}/2R_c < 0.5$.

According to the calculated values displayed in Table 5, it was found that the distance between attachment points, or length between PFPA units, was around 0.84 nm. The degree of overlap of each polymer loop, $L_{id}/2R_c$, was above the condition for brush formation ($L_{id}/2R_c$<0.5), with the exception of dextran and PVP 1300 kDa. Although the brush conformation is well known to confer protein resistance to polymers due to the steric repulsion effects, the dependence of our polymer architecture, or a polymer's antifouling ability, on the attachment efficiency of the PFPA units plays an important role in this system. The variation is presented in **Figure 5**, where it can be seen that significant changes in the conformation of the attached polymer only occur when efficiency reaches 20% or lower. Although a quantitative analysis of azide efficiency is difficult to study under the conditions presented here, if one considers that these chemical groups are known for their stability in the dark and at room temperature,[56,57] then it should be possible to assume that their binding efficiency is above the limit stated above.

3.2. Influence of Polymer Chemistry and Proposed Architecture on Fouling Response

In order to verify the abilities of the polymers tested in this work to withstand fouling, five assays covering different length scales were performed: protein resistance (3–20 nm) was analyzed both in situ and ex situ and exposure to two strains of marine bacteria (2–3 µm long) and zoospores of *U. linza* (diameter 4–6 µm at widest point of motile pyriform-shaped spore) was carried out (see Table 4 and Figure 4).

In terms of protein resistance, the ex situ ellipsometry technique showed that the best performance was obtained by PEG and hydroxylated chemistries. However, since the uptake variability often lay within the instrumental error, another technique was needed in order to confirm this set of data. In situ QCM-D was used and the experimental results obtained confirm that both dextran and PVA have very low protein uptake, supporting the information already provided by ellipsometry. A reason for this is the presence of OH groups in the latter polymers. These polymers will therefore be more likely to form a tightly bound water layer when

Table 5. Physicochemical properties of the model surfaces used assuming 100% PFPA binding efficiency (Eff = 1).

	Grafting density [nm^2]	Monomer density [nm^{-2}]	σ_{attach}	LL_i [nm]	L_{id} [nm]	R_c [nm]	$L_{id}/2R_c$
PAAm-g-PFPA	0.067	1.65	-	-	-	-	-
PVA 27 kDa	0.028	16.9	59.8	2.6	0.84	0.51	0.82
PEG 20 kDa	0.141	64.2	11.7	17.1		0.83	0.51
Dextran 2000 kDa	0.003	42.4	480.3	16.7		1.01	0.41
PEOXA 50 kDa	0.009	4.4	189.6	1.0		0.45	0.93
PVP 55 kDa	0.026	12.8	63.7	1.9		0.65	0.64
PVP 1300 kDa	0.007	77.3	250.0	11.7		1.19	0.35

σ_{attach}: attachment density; LL_i: average loop length; L_{id}: average distance between attachment points; R_c: coiled radius; $L_{id}/2R_c$: degree of overlap between loops.

compared to the nitrogen-containing polymers. This consequently results in an improved protein resistance due to a more significant physical and energetic barrier being formed.[7] The high-molecular-weight PVP data, which implies full protein resistance, suggests that other parameters, such as mechanical stiffness (or lack of it), can equally affect the nonfouling performance of a polymeric film. The negative protein uptake that characterized PEG (due to loss of film mass) may be an indication that this specific coating is not stable, especially on the time scale over which these assays were performed. Some assays could take several hours, which contrasts with the few minutes needed to perform an ellipsometric analysis and such differences therefore influence the final outcome.

Regarding the other bioassays, spores of *U. linza* and the two strains of bacteria showed a higher settlement (attachment) on the slightly more hydrophobic surfaces (PAAm-g-PFPA, advancing contact angle of 70 ± 1°). Indeed, it has been observed that zoospores typically settle in higher numbers on hydrophobic surfaces and in lower numbers but with higher adhesion strength on hydrophilic surfaces.[58] In the same way, it has also been demonstrated that various marine bacteria show a tendancy to attach on hydrophobic surfaces, irrespective of their surface chemistries.[59,60]

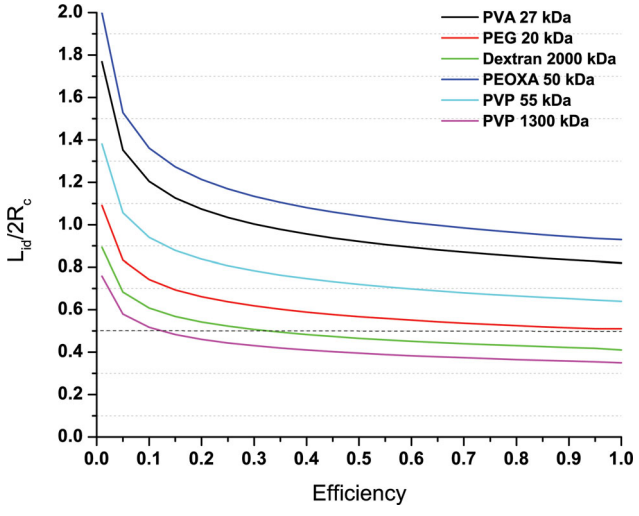

Figure 5. $L_{id}/2R_c$ variation with adhesion promoter efficiency.

However, regarding levels of settlement, different results were obtained for each species. While the two bacteria showed minimum settlement on the PEG-coated samples, spores settled in higher numbers on this sample compared to all the other nonfouling surfaces, which can be attributed to the lack of resistance of this specific coating towards the adhesives secreted by this species during the settlement process.[39] Both for spores of *U. linza* and cells of *C. marina,* settlement on the hydroxylated chemistries was minimal, which is in good agreement with the literature, which suggests that hydration is also an important parameter in achieving decreased settlement/attachment for these specific species.[6] Nevertheless, this latter hypothesis does not appear to hold for the results obtained for *M. hydrocarbonoclasticus*. Here, the lowest settlement was observed on samples coated with PEG, PEOXA, and PVP 55 kDa, while PVA, PVP 1300 kDa, and dextran showed considerably higher settlement (over 50% more than the low-settlement coatings). Dextran was the only "nonfouling" surface that showed a higher settlement of bacteria than bare SiO_2, showing that, for this specific strain of bacteria, dextran cannot be regarded as a fouling-resistant polymer. The preference of this bacterium for hydroxylated chemistries strongly suggests that hydration does not prevent its settlement. Instead, the presence of hydroxyl groups appears to play a key role in this process. The conditions under which bacteria are cultured play a major role in cell physiology and the composition of extracellular polymeric substances produced, which determine how cells respond to surfaces[61–63] *M. hydrocarbonoclasticus* is known to produce wax esters (in EPS, extracellular polymeric substances) from alcohols by oxidation via the enzyme alcohol dehydrogenase.[64] This might be a reason for the preferential settlement of *M. hydrocarbonoclasticus* on hydroxylated chemistries, in contrast to *C. marina*, which is not known to produce this enzyme. Overall, these findings suggest that hydrophilicity, or surface energy, cannot be the sole responsible parameter for the adhesion of bacteria, which is consistent with previously reported results.[45,62,65] Instead, since it is known that bacteria such as *E. coli*[66] degrade dextran, one could postulate that the same happens with *M. hydrocarbonoclasticus,* hence explaining the preferential settlement on this polysaccharide. Interestingly, the bacterium seems to attach preferentially to high-molecular-weight PVP 1300 kDa when compared to the low-molecular-weight PVP 55 kDa. The reason for the greater

resistance of the lower-molecular-weight PVP indicates that *M. hydrocarbonoclasticus* attachment might also be regulated by other parameters, such as mechanical stiffness of the polymer substrate.

One other parameter this study allows us to evaluate is the polymer conformation of the developed organic films. As calculated, only dextran and PVP 1300 kDa were characterized as having a $L_{id}/2R_C$ <0.5 (i.e., brush), while all the others were above this limit in the collapsed state but still below 1. According to the literature, a more fouling-resistant performance is associated with polymers with $L_{id}/2R_g$<1[50] when they start to adopt a brush conformation. If one considers R_g>R_c, then once the polymers are hydrated they should all readily adopt a brush-like conformation. By analyzing Figure 4, the surface that presents the most consistent resistance to proteins and all tested organisms is the one that was functionalized with PVP 55 kDa. This indicates that, while conformation and chemistry may play a key role in a polymer's resistance to biofouling, other additional physicochemical factors are equally important in conferring this ability.

All the findings stated above illustrate the complexity involved in marine biofouling but also indicate that the response of organisms to a particular surface chemistry is highly dependent on the test organism. There is no single property that will dictate the fouling performance of a coating, but rather a combination of several properties. Chemistry can help to increase resistance to fouling but cannot prevent it alone, thanks to the high adaptability of living organisms.

4. Conclusions

The adhesion promoter described in this paper provides a versatile approach to the functionalization of surfaces with a variety of polymers in a reliable and reproducible manner. By manipulating the stoichiometry of the adhesion promoter, grafting densities of the immobilized polymers and their conformational properties can be precisely tuned, enabling the impact of these properties on function to be readily studied. We have used this approach to test a range of hydrophilic uncharged polymers both against proteins and some of the most important marine-fouling test organisms.

The adhesion promoter possesses the ability to electrostatically bind to negatively charged substrates and, upon activation, covalently bind polymers in its close proximity. Validation of the functionalization method was achieved by means of different surface characterization techniques, such as dynamic contact angle, ellipsometry, and XPS. Often, our nonfouling, coated surfaces were found to decrease protein uptake to such an extent that the experimental values were below the sensitivity of the instrument used, making it difficult to state which was the best-performing nonfouling chemistry. It was shown that the response to surface chemistry by marine fouling organisms strongly depends on the organism tested and cannot be simply related to a key property, or deconvoluted into general physicochemical conditions. PVP 55 kDa showed a more consistent resistance against all biological assays performed. Although it did not match PEG's low values for protein and bacteria attachment, it showed a higher stability and less variability in the results and should be considered as a promising candidate for nonfouling surfaces.

5. Experimental Section

Substrates: Silicon wafers were purchased from POWATEC GmbH, Hünenberg, Switzerland. Two sizes were used: 10 mm × 9 mm and 76 mm × 26 mm, the latter being solely used for biological assessment (Section 2.7).

Reagents: The following materials were purchased from Sigma-Aldrich (Switzerland) and used as received: poly(allylamine hydrochloride) (PAAm·HCl, average M_w = 15 000 g mol^{-1}), poly(ethylene glycol) (PEG, average M_n = 20 000 g mol^{-1}), poly(2-ethyl-2-oxazoline) (PEOXA, average M_w = 50 000 g mol^{-1}), poly(vinyl alcohol) (PVA, average M_w = 27 000 g mol^{-1}), poly(vinyl pyrrolidone) (PVP, average M_w = 55 000 and 1 300 000 g mol^{-1}), calcium chloride dihydrate (≥99.5%), and magnesium chloride hexahydrate (≥99%). 4-(2-hydroxyethyl)piperazine-1-ethane sulfonic acid (HEPES, ≥99%) was acquired from BDH Biochemical (Switzerland) and dextran T200 (M_w = 2 000 000 g mol^{-1}) was purchased from Pharmacosmos (Denmark). Ethanol (≥99.9%), toluene (≥99.9%), 2-propanol (≥99.8%), potassium carbonate (K_2CO_3, ≥99%), sodium chloride (NaCl, ≥99.5%), sodium sulfate (Na_2SO_4, ≥99%), and potassium chloride (KCl, ≥99.5%) were acquired from Merck (Switzerland) and also used as received. N-hydroxysuccinimide-perfluorophenylazide was provided by SuSoS AG (Dübendorf, Switzerland) and lyophilized human serum (Precinorm U, Roche Diagnostics, Switzerland) dissolved in ASW with a final ionic strength of 0.7 M was used in the protein adsorption assays. Ultrapure water (purified with a water treatment apparatus from Millipore; ≥18.2 MΩ cm^{-1} resistivity, total organic content ≤5 ppb) was used throughout the experiments. ^{1}H NMR was performed for the polymers as received with a Bruker 300 MHz spectrometer, in order to confirm purity of the reagents.

Buffers: HEPES I: 10 mM *N*-(2-hydroxyethyl)piperazine-*N*′-(2-ethanesulfonic acid) (HEPES) (Fluka) pH was adjusted to 7.4 with NaOH. Artificial seawater (ASW): a) for all protein adsorption assays, ASW was freshly prepared according to the protocol described elsewhere[67] from a mixture of five individual salts, filtered with a 0.22 µm filter and pH adjusted to 8.2 with NaOH; b) for assays with bacteria and algae, ASW (Tropic Marin) was freshly prepared according to manufacturer's instructions, filtered with a 0.22 µm filter, and pH adjusted to 8.2 with NaOH.

Synthesis of PAAm-g-PFPA (Poly(allylamine) grafted perfluorophenylazide): PAAm-g-PFPA was synthesized according to the protocol developed by SuSoS AG (Dübendorf, Switzerland).[68] In brief, poly(allylamine hydrochloride) (6.33 mg, 6.8 × 10^{-3} mM monomer) and excess potassium carbonate (15.82 mg, 0.11 mM) were dissolved in water (1.3 mL) and boiled for a short period of time. After cooling down to room temperature, a solution of *N*-hydroxysuccinimide-perfluorophenylazide (NHS-PFPA) (5.62 mg, 1.7 × 10^{-2} mM) dissolved in ethanol (1.3 mL) was slowly added. The resulting solution was stirred overnight in the dark and the stock solution was then diluted to 100 mL with a 3:2 (v/v) ethanol/HEPES I mixture, yielding a polymer concentration of 0.1 mg mL^{-1}.

Surface Modification: Unless stated otherwise, samples were coated according to the protocol described in this section. All wafers were cleaned twice in toluene (HPLC quality, ≥99.99% (v/v), Fluka Switzerland), twice in 2-propanol (≥99.9%, Merck, Switzerland) (15 min sonication each), dried under a stream of N_2, and exposed to O_2 plasma (Diener Electronic Nano, Germany) for 2 min to remove adventitious contamination from the surface. The cleaned substrates were dipped in a 0.1 mg mL^{-1} PAAm-g(4)-PFPA solution for 30 min and subsequently rinsed twice with a solution of 3:2 (v/v) ethanol/HEPES I, once with Milli-Q, and again dried under a stream of N_2. The wafer surface was completely covered with the polymer solution and spin coating was carried out according the parameters described in **Table 6**.

Table 6. Polymer solution details and corresponding spin-coating parameters.

Chemistry	Concentration [mg mL^{-1}]	Solvent	Spin-coating parameters
PEG 20 kDa	50	75% ultrapure water 25% 2-propanol (v/v)	2000 rpm for 40 s 4000 rpm for 10 s
PVA 27 kDa	50		
PEOXA 50 kDa	50		
PVP 55 kDa	50	Ethanol	
PVP 1300 kDa	25	Ethanol	4000 rpm for 40 s 5000 rpm for 10 s
Dextran 2000 kDa	25	ultrapure water	

Surfaces were then left in the dark at room temperature for at least 15 min until completely dry and then exposed to UV-C light (254 nm, Philips TUV 11W) for 2 min. Excess non-bound polymers were removed by overnight immersion in ultrapure water. Finally, the surfaces were rinsed with fresh ultrapure water and dried under a stream of N_2. All functionalized surfaces were stored in the dark at room temperature until further use.

Surface Characterization by Ellipsometry (VASE): Thickness measurements were performed using a M-2000F variable-angle spectroscopic ellipsometer from J. A. Woollam Co (Lincoln, NE, USA). All data presented here were recorded at a wavelength range from 370 to 1000 nm using focusing lenses at 70° from the surface normal. Data were analysed with WVASE32 software using a three-layer model (Si/SiO_2/Cauchy; $A_n = 1.45$ and $B_n = 0.01$, $C_n = 0$). All measurements were performed under ambient conditions.

Surface Characterization by Dynamic Contact Angle (dCA): Surface-wettability measurements were performed by measuring advancing and receding contact angles with ultrapure water (6 µL) in a G2/G40 2.05-D from Krüss GmbH (Germany). Data were analyzed according to the "tangent method 2" with DSA 3 Version 1.72 software from the latter company.

Surface Characterization by X-ray Photoelectron Spectroscopy (XPS): Measuring conditions for XPS were as previously reported by Rodenstein et al.[69] All spectra were recorded using a PHI5000 Versa probe (ULVAC-PHI, INC., Chigasaki, Japan). The spectrometer is equipped with a 180° spherical-capacitor energy analyzer and a multichannel detection system with 16 channels. Spectra were acquired at a base pressure of 5×10^{-8} Pa using a focused, scanning monochromatic Al Kα source (1486.6 eV) with a spot size of 200 µm and 47.6 W power. The instrument was run in the FAT analyzer mode with electrons emitted at 45° to the surface normal. Pass energies used for survey scans was 187.85 and 46.95 eV for detail spectra. The full width at half-maximum (FWHM) of this setup is <0.8 eV for Ag $3d_{5/2}$.

The XPS spectra were evaluated using CasaXPS (version 2.3.12 and later). All binding energies are referenced relative to the hydrocarbon peak (from residual contamination in the case of the clean surfaces, or the $–CH_2–\mathbf{C}H_2–CH_2$-contribution of the polymers), set at a binding energy (BE) of 285.0 eV.

Normalized atomic percent (atom%) concentrations were calculated from the detail spectra of each element present on the surface, corrected by the appropriate relative sensitivity factors (RSFs), the asymmetry parameter,[70] the transmission function of the spectrometer, and inelastic mean free paths (IMFPs). The photoionization cross sections are normalized to C 1s according to Scofield,[71] except for Si 2p, where an experimentally determined factor of 1.06 was used, measured on a clean SiO_2 quartz reference material. This value is higher than the tabulated value from Scofield (0.817) and results in a better SiO_2 stoichiometry.[72]

Stability Tests: Short-term stability of the developed coatings and of the adhesion promoter were investigated via thickness variation. Ellipsometry measurements were performed before and after samples were stored for 1 h in 1 mL ASW, in BD Falcon multiwell plates at room temperature. Prior to measurements, samples were rinsed with ultrapure water and blown dry with a stream of N_2.

Protein Adsorption by Ellipsometry (VASE): Before exposure to the protein solution, the thicknesses of the samples were measured according to the procedure described in the surface characterization section using this same technique. Afterwards, they were immersed in ASW for 15 min and exposed to serum-ASW for 30 min. During incubation, samples were stored under ambient conditions without agitation. After exposure, these were rinsed with ASW or ultrapure water, dried under a stream of N_2 and analyzed.

Protein Adsorption by Quartz Crystal Microbalance with Dissipation (QCM-D): Protein interaction was studied by using a QCM-D E4 instrument and software from Q-Sense AB (Sweden). AT-cut polished crystals with a fundamental resonance of 5 MHz and SiO_2 coated were used (LOT-Oriel AG). Their functionalization was performed as described in Section 2.3.1 and all solvents used were degassed under vacuum for at least 45 min.

The modified crystals were exposed to HEPES I under a flow of 50 µL min^{-1} at 25 °C until a stable baseline was established. After this, the buffer was replaced with ASW under the same flow and temperature until a new baseline was obtained. Protein solution was then injected and incubation followed for at least 30 min with no flow, followed by sequential washing with ASW and HEPES I at the same flow rate as before. For both solvents, baselines were again obtained. Regeneration of the crystals was accomplished according to the following protocol: overnight immersion in 2% (v/v) SDS solution, 15 min sonication in toluene and 2-propanol, 30 min of UVO cleaning (UV Clean Model 135500 from Boekel Industries, Inc.), and again 15 min sonication in toluene and 2-propanol. After cleaning, the crystals were dried under a stream of N_2.

Marine Bacteria Assays: The ability to resist attachment of marine bacteria was investigated for all polymer coatings. For this assay, two well-known strains, commonly used in the field of marine fouling testing,[45] were chosen: *Cobetia marina* (*C. marina*, ATCC 25374^T, DSMZ, Germany), and *Marinobacter hydrocarbonoclasticus* (*M. hydrocarbonoclasticus,* ATCC 25374^T, DSMZ, Germany). Prior to exposure to the bacterial suspension, all surfaces were pre-equilibrated in ASW for one hour and then treated according to the protocol of Pranzetti et al.[73] Briefly, after bacteria reached a logarithmic growth phase, they were washed with ASW and centrifuged at 8000 rpm for 1 min, twice. This allowed the removal of culture medium and secreted extracellular polymeric substances (EPS). Test surfaces (three replicates per test surface) placed in individual compartments of Quadriperm dishes (Greiner Bio-One Ltd) were then exposed to 10 mL of bacterial suspension with an $OD_{600} = 0.1$ (4×10^{-7} cells mL^{-1}) for one hour, while agitating at 50 rpm on a plate shaker. After this, the bacterial suspension was replaced by 10 mL ASW and the dishes agitated for 1 min at the same rotational speed. In order to fix the bacteria, the surfaces were exposed to a solution of 2.5% (v/v) of glutaraldehyde in ASW for 20 min, washed in deionized water and then left to air-dry overnight. Before microscopic observation, the surfaces were stained with SYTO 13 (Invitrogen Molecular Probes) at 5 µM and left in the dark for 10 min. Cells were visualized using a 40× objective attached to a Zeiss epifluorescence microscope (excitation and emission λ: 450/490 and 515/565 nm, respectively) connected to the imaging analysis system AxioVision Rel. 4.8.1. For each sample, 30 fields of view were counted for each of the three replicate test surfaces. Two independent experiments were conducted with similar results. One set of data is shown in the results section.

Zoospores of Ulva linza Assays: The assay quantifies the number of spores that settle (i.e., permanently attach) to the test surfaces. All surfaces were equilibrated in ASW for one hour prior to the start of the assay. The protocol for the collection of *U. linza*, the release of spores, and the settlement assay was followed as described previously.[74] In brief, a suspension of zoospores in ASW with an $OD_{660} = 0.15$ (approx. 1×10^6 spores mL^{-1}) was prepared. 10 mL of this suspension were added to individual compartments of Quadriperm dishes, each containing a test surface (three replicates per test surface). The dishes were incubated in the dark for 45 min and then washed by passing each

sample 10 times through a beaker of ASW to remove unsettled (motile) spores. Settled spores were fixed using 2.5% (v/v) glutaraldehyde for 20 min. The surfaces were sequentially washed with ASW, 1:1 (v/v) ASW/deionized water, and deionized water. Finally, the test surfaces were allowed to air-dry and settled spores were counted by chlorophyll autofluorescence using epifluorescence microscopy (20× objective; excitation and emission λ: 546 and 590 nm, respectively) as previously described for the marine bacteria assays.

Statistical Analysis: Using the software Minitab 15, data were checked for normality and most data conformed to normality assumptions. One-way ANOVA with pairwise Tukey comparison test was then used to determine differences between the eight test surfaces. Values were considered significantly different from each other when $p < 0.05$. Means and standard deviations or standard errors of the mean are shown.

Supporting Information

Supporting Information is available from the Wiley Online Library or from the author.

Acknowledgements

This research has been funded by the European Community's 7th Framework Programme FP7/2007-2013 under Grant Agreement 237997. A.S. would like to thank Dr. Prathima Nalam and Dr. Mirren Charnley for fruitful discussions regarding QCM data interpretation and statistical analysis.

Received: November 24, 2012
Revised: April 8, 2013
Published online: June 17, 2013

[1] C. M. Magin, S. P. Cooper, A. B. Brennan, *Mater. Today* **2010**, *13*, 36.
[2] M. P. Schultz, J. A. Bendick, E. R. Holm, W. M. Hertel, *Biofouling* **2011**, *27*, 87.
[3] J. A. Callow, M. E. Callow, *Nat. Commun.* **2011**, *2*, 244.
[4] I. Omae, *Appl. Organomet. Chem.* **2003**, *17*, 81.
[5] S. Krishnan, C. J. Weinman, C. K. Ober, *J. Mater. Chem.* **2008**, *18*, 3405.
[6] S. Schilp, A. Rosenhahn, M. E. Pettitt, J. Bowen, M. E. Callow, J. A. Callow, M. Grunze, *Langmuir* **2009**, *25*, 10077.
[7] S. Chen, L. Li, C. Zhao, J. Zheng, *Polymer* **2010**, *51*, 5283.
[8] S. Jiang, Z. Cao, *Adv. Mater.* **2010**, *22*, 920.
[9] V. Zoulalian, S. Zürcher, S. Tosatti, M. Textor, S. Monge, J. Robin, *Langmuir* **2010**, *26*, 74.
[10] R. Michel, S. Pasche, M. Textor, D. G. Castner, *Langmuir* **2005**, *21*, 12327.
[11] H. S. Sundaram, Y. Cho, M. D. Dimitrou, C. J. Weinman, J. A. Finlay, G. Cone, M. E. Callow, J. A. Callow, E. J. Kramer, C. K. Ober, *Biofouling* **2011**, *27*, 589.
[12] Y. Wang, J. A. Finlay, D. E. Betts, T. J. Merkel, C. J. Luft, M. E. Callow, J. A. Callow, J. M. DeSimone, *Langmuir* **2011**, *27*, 10365.
[13] Y. Wang, L. M. Pitet, J. A. Finlay, L. H. Brewer, G. Cone, D. E. Betts, M. E. Callow, J. A. Callow, D. E. Wendt, M. A. Hillmyer, J. M. DeSimone, *Biofouling* **2011**, *27*, 1139.
[14] M. C. Woodle, C. M. Engbers, S. Zalipsky, *Bioconjugate Chem.* **1994**, *5*, 493.
[15] H. Wang, L. Li, Q. Tong, M. Yan, *ACS Appl. Mater. Interfaces* **2011**, *3*, 3463.
[16] M. Rovira-Bru, F. Giralt, Y. Cohen, *J. Colloid Interface Sci.* **2001**, *235*, 70.
[17] S. Robinson, P. A. Williams, *Langmuir* **2002**, *18*, 8743.
[18] Z. Wu, H. Chen, X. Liu, Y. Zhang, D. Li, H. Huang, *Langmuir* **2009**, *25*, 2900.
[19] K. Rasmussen, K. Østgaard, *Biofouling* **2001**, *17*, 103.
[20] T. Murosaki, T. Noguchi, K. Hashimoto, A. Kakugo, T. Kurokawa, J. Saito, Y. M. Chen, H. Furukawa, J. P. Gong, *Biofouling* **2009**, *25*, 657.
[21] K. Rasmussen, P. R. Willemsen, K. Østgaard, *Biofouling* **2002**, *18*, 177.
[22] C. Perrino, S. Lee, S. W. Chooi, A. Maruyama, N. D. Spencer, *Langmuir* **2008**, *24*, 8850.
[23] S. Martwiset, A. E. Koh, W. Chen, *Langmuir* **2006**, *22*, 8192.
[24] F. Fang, I. Szleifer, *Langmuir* **2002**, *18*, 5497.
[25] I. Szleifer, *Phys. A* **1997**, *244*, 370.
[26] J. Rühe, *Polymer Brushes: On the Way to Tailor-Made Surfaces, in Polymer Brushes: Synthesis, Characterization, Applications*, (Eds: R. C. Advincula, W. J. Brittain, K. C. Caster, J. Rühe), Wiley-VCH Verlag GmbH & Co. KGaA, Weinheim, Germany **2005**.
[27] S. Minko, *Polymer Rev.* **2006**, *46*, 397.
[28] Y. Tsujii, K. Ohno, S. Yamamoto, A. Goto, T. Fukuda, *Adv. Polymer Sci.* **2006**, *197*, 1.
[29] H. Wang, J. Ren, A. Hlaing, M. Yan, *J. Colloid Interface Sci.* **2011**, *354*, 160.
[30] H. Murata, B. J. Chang, O. Prucker, M. Dahm, J. Ruhe, *Surf. Sci.* **2004**, *570*, 111.
[31] G. L'Abbé, *Chem. Rev.* **1969**, *69*, 345.
[32] E. F. V. Scriven, *Azides and Nitrenes: reactivity and utility*, (Ed: E. F. V. Scriven), Academic Press, Orlando, Florida **1984**.
[33] S. Bräse, C. Gil, K. Knepper, V. Zimmermann, *Angew. Chem. Int. Ed.* **2005**, *44*, 5188.
[34] J. F. W. Keana, S. X. Cai, *J. Fluorine Chem.* **1989**, *43*, 151.
[35] J. F. Keana, S. X. Cai, *J. Org. Chem.* **1990**, *55*, 3640.
[36] H. Baruah, S. Puthenveetil, Y. A. Choy, S. Shah, A. Y. Ting, *Angew. Chem. Int. Ed.* **2008**, *47*, 7018.
[37] J. F. W. Keana, S. X. Cai, *J. Org. Chem.* **1990**, *55*, 3640.
[38] S. Bräse, K. Banert, *Organic Azides: Syntheses and Applications*, (Eds: S. Bräse, K. Banert), John Wiley & Sons, Wiltshire, UK **2009**.
[39] J. A. Callow, M. E. Callow, in *Biological Adhesives*, (Eds: A. M. Smith, J. A. Callow) Springer-Verlag Berlin, Heidelberg, Germany **2006**, Ch.4.
[40] F. Höök, B. Kasemo, T. Nylander, C. Fant, K. Sott, H. Elwing, *Anal. Chem.* **2001**, *73*, 5796.
[41] E. Reimhult, C. Larsson, B. Kasemo, F. Höök, *Anal. Chem.* **2004**, *76*, 7211.
[42] F. Höök, J. Vörös, M. Rodahl, R. Kurrat, P. Boni, J. J. Ramsden, M. Textor, N. D. Spencer, P. Tengvall, J. Gold, B. Kasemo, *Colloids Surf. B* **2002**, *24*, 155.
[43] K. D. Kwon, H. Green, P. Bjöörn, J. Kubicki, *Environ. Sci. Technol.* **2006**, *40*, 7739.
[44] J. J. I. Ramos, S. E. Moya, *Macromol. Rapid Commun.* **2011**, *32*, 1972.
[45] T. Ekblad, G. Bergström, T. Ederth, S. L. Conlan, R. Mutton, A. S. Clare, S. Wang, Z. Liu, Q. Zhao, F. D'Souza, G. T. Donnelly, P. R. Willemsen, M. E. Pettitt, M. E. Callow, J. A. Callow, B. Liedberg, *Biomacromolecules* **2008**, *9*, 2775.
[46] S. Han, C. Kim, D. Kwon, *Polymer* **1997**, *38*, 317.
[47] W. Hartung, T. Drobek, S. Lee, S. Zürcher, N. D. Spencer, *Tribol. Lett.* **2008**, *31*, 119.
[48] P. Pincus, *Macromolecules* **1991**, *24*, 2912.
[49] G. Greene, G. Yao, R. Tannenbaum, *Langmuir* **2004**, *20*, 2739.
[50] G. L. Kenausis, J. Vörös, D. L. Elbert, N. Huang, R. Hofer, L. Ruiz-Taylor, M. Textor, J. A. Hubbell, N. D. Spencer, *J. Phys. Chem. B* **2000**, *104*, 3298.
[51] L. Feuz, F. A. M. Leermakers, M. Textor, O. Borisov, *Langmuir* **2008**, *24*, 7232.
[52] T. Matsuda, G. D. Smith, R. G. Winkler, D. Y. Yoon, *Macromolecules* **1995**, *28*, 165.

[53] K. S. Iyer, I. Luzinov, *Macromolecules* **2004**, *37*, 9538.
[54] R. L. Jones, R. J. Spontak, *J. Chem. Phys.* **1995**, *12*, 5137.
[55] M. Fritsche, D. W. Heerman, M. Dutra, C. E. Cordeiro, *Macromol. Theory Simul.* **2010**, *19*, 440.
[56] S. A. McMahan, R. R. Burgess, *Biochemistry* **1994**, *33*, 12092.
[57] R. J. Griffin, *Prog. Med. Chem.* **1994**, *31*, 121.
[58] S. Schilp, A. Kueller, A. Rosenhahn, M. Grunze, M. E. Pettitt, M.E. Callow, J. A. Callow, *Biointerphases* **2007**, *2*, 143.
[59] M. Samuelsson, D. L. Kirchman, *Appl. Environ. Microbiol.* **1990**, *56*, 3643.
[60] K. M. Wiencek, M. Fletcher, *J. Bacteriol.* **1995**, *177*, 1959.
[61] D. P. Bakker, B. R. Postmus, H. J. Busscher, H. C. van der Mei, *Appl. Environ. Microbiol.* **2004**, *70*, 3758.
[62] T. Ederth, T. Ekblad, M. E. Pettitt, S. L. Conlan, C. Du, M. E. Callow, J. A. Callow, R. Mutton, A. S. Clare, F. D'Souza, G. Donnelly, A. Bruin, P. R. Willemsen, X. J. Su, S. Wang, Q. Zhao, M. Hederos, P. Konradsson, B. Liedberg, *ACS Appl. Mater. Interfaces* **2011**, *3*, 3890.
[63] H. H. Tuson, D. B. Weibel, *Soft Matter* **2013**, *9*, 4368.
[64] E. Holtzapple, C. Schmidt-Dannert, *J. Bacteriol.* **2007**, *189*, 3804.
[65] C. Liu, Q. Zhao, *Biofouling* **2011**, *27*, 275.
[66] N. Argibay, C. Perrino, M. Rimann, S. Lee, N. D. Spencer, *Lubrication Sci.* **2009**, *21*, 415.
[67] A. L. Cordeiro, R. Zimmermann, S. Gramm, M. Nitschke, A. Janke, N. Schäfer, K. Grundke, C. Werner, *Soft Matter* **2009**, *5*, 1367.
[68] S. Zürcher, S. Tosatti, A. Dorcier, S. Fusco, I. Lopez, *Eur. 2 236 524*, **2010**.
[69] M. Rodenstein, S. Zürcher, S. G. P. Tosatti, N. D. Spencer, *Langmuir* **2010**, *26*, 16211.
[70] R. F. Reilman, A. Msezane, S. T. Manson, *J. Electron Spectrosc. Relat. Phenom.* **1976**, *8*, 389.
[71] J. H. Scofield, *J. Electron Spectrosc. Relat. Phenom.* **1976**, *8*, 129.
[72] M. Crobu, A. Rossi, F. Mangolini, N. D. Spencer, *Anal. Bioanal. Chem.* **2012**, *403*, 1415.
[73] A. Pranzetti, S. Salaün, S. Mieszkin, M. E. Callow, J. A. Callow, P. M. Mendes, *Adv. Funct. Mater.* **2012**, *22*, 3672.
[74] I. Thome, M. E. Pettitt, M. E. Callow, J. A. Callow, M. Grunze, A. Rosenhahn, *Biofouling* **2012**, *28*, 501.
[75] C. H. Choi, J. E. Zuckerman, P. Webster, M. E. Davis, *Proc. Natl. Acad. Sci. USA* **2011**, *108*, 6656.
[76] C. M. Papadakis, R. Ivanova, K. Lüdtke, K. Mortensen, P. K. Pranzas, R. Jordan, *J. Appl. Crystallogr.* **2007**, *40*, s361.
[77] J. Piehler, A. Brecht, K. Hehl, G. Gauglitz, *Colloids Surf. B* **1999**, *13*, 325.
[78] B. J. Lommerts, D. J. Sikkema, *Macromolecules* **2000**, *33*, 7950.
[79] J. Pei, H. Hall, N. D. Spencer, *Biomaterials* **2011**, *32*, 8968.
[80] K. D. F. Vlugt-Wensink, T. J. H. Vlugt, W. Jiskoot, D. J. A. Crommelin, R. Verrijk, W. E. Hennink, *J. Controlled Release* **2006**, *111*, 117.